NEUTRON AND GAMMA PROBES: THEIR USE IN AGRONOMY

O.O.S. Bacchi[1,4]; K. Reichardt[2,4]; M. Calvache[3]; L.C. Timm[1,5]

1.Introduction

Agriculture is carried out on a very thin soil layer of the earth, as compared to the dimensions of the atmosphere or geosphere. In spite of its slim dimension, soil is indispensable for life on continents, being the medium for growth of essential autotrophic plants, which produce food and fiber for humans and animals. Without soil, our planet would not be green and all life would be restricted to the oceans.

Soil is an important reservoir of fresh water. Soil transforms discontinuous precipitation into continuous discharges recognized as streams and rivers and continuous flow of water to the roots of plants. The retention capacity of the soil, able to sequester rainwater, is approximately the same order of magnitude of the capacity of all lakes. Moreover, the amount of stored water in soil equals one-third of all fresh water in lakes (including artificial reservoirs) and is larger than that of riverbeds. Soil water together with ground water exceeds more than two orders of magnitude all surface fresh water.

Ultimately, all the studies in soil hydrology have a unique aim – a better understanding and description of hydrological processes. The individual elementary processes of infiltration, redistribution, drainage, evaporation and evapotranspiration are first analyzed and subsequently considered in combination during a particular sequence of events or season. Transport of solutes is also considered as an integral part of those processes. A proper physical understanding of them requires several levels of approximate studies. One study level considers the characterization and quantification of processes for real soils, i.e. field soils, often called “point scale” studies (Kutilek & Nielsen, 1994).

The studies of such processes, which occur in the soil porous system, require detailed characterization of the three soil system components: solid, liquid and gaseous phases.

---

[1]Soil Physics Laboratory, CENA/USP, Piracicaba, Brazil

[2]Department of Exact Sciences, ESALQ/USP, Piracicaba, Brazil

[3]University of Ecuador, Quito, Ecuador

[4]CNPq fellow

[5]FAPESP fellow

The solid phase is represented by the soil particles, which vary considerably from soil to soil in quality, size and arrangement. In terms of quality, the particles are divided in two groups: organic and mineral matters. The organic part can be fresh, partially decomposed or decomposed into humus. The composition of the mineral part depends on the parent material that formed the soil. Its major components are SiO_4, Al_2O_3, Fe_2O_3, CaO, MgO, K_2O, P_2O_5. Several components are responsible for the presence of the essential elements for plant growth and development, and for most of the 92 natural elements of Earth's crust.

The size of the particles is evaluated by soil mechanical analysis, which, in most cases ranks them in three main groups: sand (from 0.05 mm to 2 mm), silt (from 0.002 mm to 0.05 mm) and clay (<0.002 mm). The content of these three fractions define the soil texture, used to classify soils, e.g. silt-loam, clay-loam, sandy-clay. The arrangement of these particles defines the soil structure, the packing of the solid material that also defines the empty or porous space, occupied either by water or air. One very important soil attribute, related to the solid phase is the bulk density, which is the mass of solid material contained per unit bulk volume of soil. The soil bulk density is inversely related to the soil porosity and, therefore, important in compaction and aeration problems.

The liquid phase, in general called soil water, is a diluted aqueous solution, containing a wide variety of ions, salts and molecules including organic ones. It represents the pool of essential nutrients for plant growth and development, and is continuously renewed by physical-chemical interactions between soil particles, water and gases. The liquid phase is quantified as soil water content, which is the mass or volume of water per mass of dry soil or per volume of bulk soil. In a soil profile, soil water contents are integrated in depth, representing then the so-called water storage.

The amounts of water in the soil vary extensively from situation to situation. The soil reservoir is filled by rainfall, irrigation or snow melting, and is emptied by evaporation, transpiration and drainage to deeper zones. In Agronomy, a useful range of soil water content is defined as available water, the water that can be used by plants and of extreme importance for crop production. In cases of low water availability, irrigation complements the needs of the crops, and in cases of excess, drainage projects eliminate the excess of water.

Soil air is very important for the supply of oxygen to the living organisms of the soil, including plant roots. Soil aeration depends on the porous space of the soil and of the percentage filled with water. An ideal soil has 50 % of its volume occupied by solids, 25 % by

water and 25 % by air.

It is not the intention of the authors to cover here the study of the processes that occur in the soil, for which more detailed available textbooks and related journals are recommended. The present text is restricted only to the use of two nuclear techniques, very suitable for "point scale" studies, related to the soil porous system characterization: neutron moderation and gamma radiation attenuation methods, for the measurement of soil water content and soil bulk density.

1.1. Soil Water Content and Bulk Density

Soil water content, although being a very simple soil physics concept, is very difficult to be evaluated in the field. Estimates of soil water content obtained through many methods often deviate considerably from the "true" value, which in reality, is never known. The main problem lies in sampling procedures. Once a soil sample is taken from the field and brought to the laboratory, its soil water content can be estimated with a high degree of precision and accuracy. It is, however, never known if the collected sample really represents the soil at the desired depth, mainly due to soil variability and sampling procedures.

Soil water content can be estimated on a weight or a volume basis. In this work we will use the following symbols and definitions:

a) soil water content by weight w [(g H_2O)·(g dry soil)$^{-1}$]

$$w = \frac{\text{mass of water}}{\text{mass of dry soil}} = \frac{m_w - m_d}{m_d} \tag{1}$$

where m_w = mass of wet soil and m_d = mass of dry soil.

b) soil water content by volume θ [(cm^3 H_2O)·(cm^3 of bulk soil)$^{-1}$]

$$\theta = \frac{\text{volume of water}}{\text{bulk volume of soil}} = \frac{m_w - m_d}{V} \tag{2}$$

where V is the volume of the soil sample. In this definition it is assumed that the density of water is 1 g·cm^{-3} and, therefore, (m_w - m_d) is equal to the volume of water. It can be shown that

$$\theta = w \cdot \rho_b \qquad (3)$$

where ρ_b is the bulk density of the dry soil [(g dry soil)·(cm^3 of bulk soil)$^{-1}$] defined by:

$$\rho_b = \frac{m_d}{V} \qquad (4)$$

Example: In a soil profile, a soil sample was collected at the depth of 20 cm, with a volumetric cylinder of 200 cm^3 and 105.3 g. After handling the sample in the laboratory, eliminating all excess of soil from the outside of the cylinder and being sure that the soil was occupying the volume V of the cylinder, the sample weighed 395.6 g. After the sample was dried in a ventilated oven at 105^{o}C to a constant weight, its final mass was 335.7 g. In this case:

$$w = \frac{395.6 - 335.7}{335.7 - 105.3} = 0.260\ \text{g} \cdot \text{g}^{-1} \text{ or } 26\% \text{ by weight}$$

$$\theta = \frac{395.6 - 335.7}{200} = 0.300\ \text{cm}^3 \cdot \text{cm}^{-3} \text{ or } 30\% \text{ by volume}$$

$$\rho_b = \frac{335.7 - 105.3}{200} = 1.152\ \text{g} \cdot \text{cm}^{-3}$$

and, according to equation (3): 0.300 = 1.152[(g dry soil)·(cm^3 of bulk soil)$^{-1}$]·0.260[(g H_2O)·(g dry soil)$^{-1}$].

There are several methods for the determination of soil water content and bulk density. They differ mainly in the form of sampling, but equations (1) through (4) are always

applicable when information is available. The greatest difficulty lies in the measurement of *V*. Because sampling soil with a simple auger destroys the structure of the soil, information about *V* is lost. In this text we will not discuss all these "classical" methods of soil water measurement. The reader is referred to any basic soil physics text, or specifically to "Methods of Soil Analysis", part I, American Society of Agronomy, Monograph 9 (Klute,1986).

One great disadvantage of the classical methods is their destructive feature. With each destructive sampling event, the soil profile is severely damaged. Even sampling with a simple auger, several samplings destroys a small plot. Soil variability presents an additional problem. For each sampling event, collecting soil at the "same" depth requires another location to be sampled. A third problem, which might be minor, is the time required for oven-drying each sample. Minimal drying times are at least 24 h.

With the use of neutron probes, which we will discuss in detail in the following pages, we cause little disturbance to the soil profile. Only once is it necessary to introduce an access tube to a desired soil depth, and thereafter, measurements can be taken repeatedly at any depth or time in a matter of minutes. Of course, there are also disadvantages in the use of neutron probes. At the end of this text we will discuss advantages and disadvantages of their use.

2. Depth Neutron probes

2.1. Instrument Description and Working Principle

A neutron probe consists essentially of two parts: (1) shield with probe, and (2) electronic counting system. In some models these parts are separable and in others not.

2.1.1. Shield with Probe

The probe is a sealed metallic cylinder 3 to 5 cm in diameter and 20 to 30 cm in length. It contains a radioactive source that emits fast neutrons, a slow neutron detector and a pre-amplifier. The signal of the pre-amplifier goes through a 5 to 20 m long cable to the electronic counting system.

The geometry of the probe, type and activity of the neutron source, type of detector

and pre-amplifier vary considerably depending upon the particular manufacturer. Neutron sources are a mixture of an alpha particle emitter (like americium and radium) and a fine powder of beryllium. When alpha particles bombard beryllium nuclei, the following reaction takes place:

$$^{4}_{2}\alpha + ^{9}_{4}\mathrm{Be} \rightarrow ^{1}_{0}\mathrm{n} + ^{12}_{6}\mathrm{C}$$

The neutrons, which are a product of the reaction have energies in the range of 0 to 10 MeV, (1 eV = $1.6 \cdot 10^{-19}$ J) with an average value of about 2 Mev (fast neutrons).

The strength of the sources is generally given by the activity of the alpha emitter, in milliCuries (mCi) or in Becquerel (Bq). Most sources have an activity in the range of 5 to 50 mCi. Because most alpha emitters also emit some gamma radiation, most sources generally emit alpha particles, gamma radiation and fast neutrons. Therefore, radiation protection is an important issue. The shield, which is the container for the probe, has to be properly designed to protect the user from the radiation. Commercially manufactured probes stored in a shield exposes the user only to permissible levels of radiation.

The user is exposed to gamma radiation and fast neutrons if the probe is not in the protection shield. <u>Such exposure should be absolutely avoided</u>. The design of the shield and probe allows the probe to leave the shield and pass immediately into the soil completely avoiding excessive radiation exposure.

Gamma radiation is most efficiently shielded by lead. Fast neutrons are shielded by paraffin, polyethylene or any other material with a high content of hydrogen. Hence, neutron probe shields are generally made of lead and a hydrogen-containing material.

During measurements, the probe is lowered to the desired depth in the soil, inside of an aluminum access tube. Because aluminum is “transparent” to fast neutrons, they are scattered by the soil within a distance of 30 to 50 cm from the source. As a result of this scattering, fast neutrons lose energy and are slowed. This interaction within the soil profile is used to estimate soil water content, as will be seen later.

Next to the source is a slow neutron detector. This detector counts only slow neutrons,

not fast neutrons. There are several slow neutron detectors available, e.g. boron tri-fluoride detectors, ^{3}He detectors, and scintillation detectors. Each manufacturer makes its choice because all detectors have both advantages and disadvantages.

The pulses coming from the detector are first pre-amplified in the probe. Only these pre-amplified pulses are sent to the electronic counting system through the cable that connects the two parts of the neutron probe.

2.1.2. Electronic Counting System

Electronic counting systems vary according to probe type. Nevertheless, each essentially consists of an amplifier, a high-voltage source, a counter, a timer, rechargeable batteries and a microprocessor. Inasmuch as counting time is related to the statistical accuracy of estimating the soil water content, most probes have several counting options. With each count corresponding to an impulse originating from one slow neutron reaching the detector, the micro-processor converts the raw count data into counts per minute (cpm) or counts per second (cps).

Present-day neutron probes have micro-processors which utilizes calibration equations supplied by the user for several soils, and the results are given directly in soil water content (%, $g \cdot g^{-1}$, $cm^{3} \cdot cm^{-3}$) for each depth and location, or in terms of the water stored in a given soil layer [$(mm\ H_2O) \cdot (10\ cm\ of\ soil)^{-1}$] or profile.

Because each manufacturer provides operational instructions for their neutron probe, such details will not be discussed here. Figure 1 is a schematic diagram of a depth neutron probe being used in the field for measuring the soil water content at a particular depth below the soil surface.

The working principle of neutron probes is simple and straightforward. The neutron source emits fast neutrons, which interact with soil particles and soil water that surrounds the probe. Since neutrons have no charge, the electric fields associated with the charged soil particles do not affect their movement. Three processes occur during this interaction: neutron absorption by nuclei, neutron scattering through collisions, and neutron disintegration.

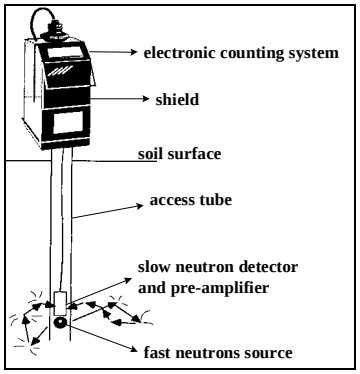

Figure 1 –Depth neutron probe diagram at working position (Source: 503 DR Hydroprobe - CPN - Operating Manual)

Neutron absorption by nuclei depends very much on the energy of the neutron and the particular target nucleus. The "probability" of this process is measured through the cross section of the reaction that, in general, for most of the elements present in soils, is very low. If the reaction occurs, one neutron is absorbed by a nucleus ${}^{A}_{Z}X$, according to:

$$ {}^{1}_{0}n + {}^{A}_{Z}X \rightarrow {}^{A+1}_{Z}X $$

where the new nucleus ${}^{A+1}_{Z}X$ is, in some cases, unstable and disintegrates emitting radiation. This is the same principle of neutron activation. The process, however, occurs only with a few nuclei present in soils, (e.g., Ag, Au, In, Fe, Al, and Mn)**.** In most soils these nuclei are present in very low concentrations. Also, because the neutron flux emitted by the source has generally a very low intensity, the probability of a neutron capture is extremely low. In many cases ${}^{A+1}_{Z}X$ is stable (e.g. ${}^{12}_{6}C + {}^{1}_{0}n \rightarrow {}^{13}_{6}C$; ${}^{14}_{7}N + {}^{1}_{0}n \rightarrow {}^{15}_{7}N$), and in the cases it is radioactive (e.g., ${}^{23}_{13}Al + {}^{1}_{0}n \rightarrow {}^{24}_{13}Al$ with a half-life of 2.3 minutes), most half-lives are generally very short. Owing to these facts, there is virtually no activation of soil material when a neutron probe is placed into the soil. Moreover, the aluminum access tubes, which might become slightly radioactive during one measurement decays in only a few minutes.

Neutron scattering by elastic and non-elastic collisions is the most important process on which the working principle of the neutron probe is based. Through collisions, fast neutrons (high energies > 2 MeV) loose energy (moderation) and become slow or thermal

neutrons (low energies < 0.025 eV). As illustrated in Table 1, if collisions are elastic, the heavier the target nucleus the less energy is lost by the neutron.

Because ^{1}H is the most efficient target atom for reducing neutron energy, it is said that hydrogen is a good neutron moderator. And because hydrogen is a constituent of water, water is also a good neutron moderator. Hence, in a given soil, the wetter the soil, the greater the number of slow neutrons in the presence of a fast neutron source. With the exception of soil organic matter, which may indeed gradually fluctuate with time, other soil materials containing hydrogen remain constant and are taken into account during calibration.

Table 1

Number of elastic collisions necessary to reduce the energy of a neutron from 2 MeV to 0.025 eV

Target Isotope	Number of Collisions
^{1}H	18
^{2}H	25
^{4}He	43
^{7}Li	68
^{12}C	115
^{16O}	152
^{238}U	2172

Free neutrons are unstable and disintegrate with a half-life of 13 min. Hence, if a free neutron is not captured it will eventually disintegrate according to:

$$^{1}_{0}n \rightarrow {}^{1}_{1}p + \beta^{-} + \nu + 780\text{Kev}$$

where $^{1}_{1}p$ = proton; β^{-}= beta particle and ν = neutrino.

When the probe is lowered into the access tube, a stable, spherical “cloud” of slow neutrons quickly develops in the soil around the source having a diameter of about 30 cm. The drier the soil, the greater the diameter of the cloud. The number of slow neutrons per unit volume at each point of the cloud remains constant and is proportional to the water content of the soil within the cloud. Since the slow neutron detector is placed inside the cloud volume,

the count rate (cpm or cps) is proportional to the soil water content θ of the same volume. The instrument is calibrated with samples of known θ. More details about neutron moisture meter theory can be found in Greacen (1981) and IAEA (1970).

2.2. Safety and Maintenance

2.2.1. Safety Standards for Protection Against Ionizing Radiation and for the Safety of Radiation Sources.

The rules and standards that control the use and disposal of radioactive materials are established at an international level by the IACRS (Inter-Agency Committee on Radiation Safety) which co-ordinates the activities of related international organizations. The standard rules are published by IAEA in the publication "IAEA Safety Series", and involve the following aspects: security fundamentals, standards and rules of security, safety procedures related to nuclear safety and radiation protection, including the management of radioactive disposal. The most recent publication is IAEA *Safety Series No. 115-I : International Basic Safety Standards for Protection Against Ionizing Radiation and for the Safety of Radiation Sources (IAEA, 1994).*

It is important to mention that each country has its own organization that deals with these subjects at a local level, defining the regulation and the inspection of the use of radioactive materials. Due to this fact, details or license for its use, security rules for operation, and transport and storage of nuclear equipment such as neutron or gamma probes have to follow the recommendations of these organizations in each specific country.

Therefore, in this section, only basic and general aspects related to radiation and the security of the use of radioactive materials will be covered. The user should consider these aspects as well as those available internationally or locally.

2.2.2. Basic Concepts and Security Aspects for Radioactive Source Handling

2.2.2.1. Radioactivity

The atomic nucleus is composed of positively charged particles, the protons, and neutral particles, the neutrons, which interact among themselves by different kinds of forces: electrical, gravitational, and nuclear. The equilibrium of these forces depends on the proportion between the number of protons (Z = atomic number) and the number of neutrons (N), present in the nucleus, and defines the condition of nuclear stability. This proportion defining the stability of a nucleus is not constant for all atoms, and depends on the mass number ($A = Z + N$) according to the empirical relation:

$$Z = \frac{A}{2 + 0.0146A^{2/3}}.$$

Hence, a given atom may be unstable or radioactive due to an excess of protons (Z much larger than N) or due to an excess of neutrons (N much larger than Z), presenting a natural tendency for the establishment of an equilibrium through different types of transformations. Here, we present two examples related to neutron probes.

a) Neutron source – a mixture of americium and beryllium isotopes

Americium, an unstable isotope having an excess of protons (Z/N = 95/146 = 0.65), tends toward equilibrium by emitting an alpha particle of energy 5.48 MeV and a gamma-ray of 60 KeV, according to:

$$^{241}_{95}Am \rightarrow {}^{237}_{93}Np + {}^{4}_{2}\alpha + E$$

Compared to americium, the resulting isotope of neptunium has a smaller excess of protons with a smaller Z/N ratio of 0.64. Neptunium is also unstable and subsequent transformations occur until equilibrium is reached.

Beryllium, the other constituent of the mixture, contains an excess of neutrons (Z/N = 0.8) and reacts with the alpha particle emitted from the americium according to:

$$^{9}_{4}Be + ^{4}_{2}\alpha \rightarrow ^{13}_{6}C \rightarrow ^{12}_{6}C + ^{1}_{0}n + E$$

Compared to $^{9}_{4}Be$, the new isotopes $^{13}_{6}C$ and $^{12}_{6}C$ have smaller excesses of neutrons with higher *Z/N* ratios (*Z/N* = 0.86 and *Z/N* = 1, respectively). The isotope $^{13}_{6}C$ is unstable and by emitting a fast neutron transforms into $^{12}_{6}C$.

b) Gamma-ray source – an isotope of cesium

The unstable isotope $^{137}_{55}Cs$ with an excess of neutrons (*Z/N* = 0.67) transforms according to:

$$^{137}_{55}Cs \rightarrow ^{137}_{56}Ba \rightarrow ^{137}_{56}Ba + \beta^{-} + \gamma(661.6\ \text{Kev})$$

In this reaction the stable isotope of barium is produced either by the emission of a β^{-} particle having an energy of 1176 KeV or mainly by the emission of a β^{-} particle having an energy of 514 KeV followed by an emission of gamma radiation having an energy of 661.6 KeV.

If a probe contains both neutron and gamma ray sources, it is understood from the above reactions that four types of radiation are emitted: α, β, γ and neutrons. The main characteristics of this radiation are described in the item 2.2.2.3

2.2.2.2. Radioactivity Units of Radioactive Sources

In general, the quantity of a radioactive material is measured in relation to its activity, which represents the number of atoms under disintegration per unit of time. Earlier, the most commonly used unit of radioactivity was the Curie (Ci) which is based on the decay rate of radium (Ra). One Ci is equivalent to $3.7 \cdot 10^{10}$ disintegration per second. Today, the internationally adopted standard unit for radioactivity is the Becquerel (Bq), corresponding to one disintegration per second. Hence, 1 Ci = $3.7 \cdot 10^{10}$ Bq.

2.2.2.3. General Characteristics of Radiations

Table 2 provides some comparative characteristics of the four types of radiation associated with neutron and gamma ray probe. If one considers protection from the radiation during the handling of such a probe, the main concern has to be devoted to the neutrons and the gamma radiation because the alpha and beta radiation is sufficiently attenuated by the metal capsule sealing the two sources.

Because neutrons have no charge, their penetration power is very large. They can penetrate and completely pass through a human body. During their penetration they transmit all or part of their kinetic energy causing damage to tissues and organs. Because of this large penetration power, the value of their RBE varies from 5 to 10 for energies of 0.025 eV (slow neutrons) to 10 MeV (fast neutrons), respectively. This means that for the same exposure doses measured in RAD (Radiation Absorption Dose) for gamma radiation and for neutrons, the damage of the human body caused by neutrons is 5 to 10 times greater than that by gamma radiation. With the shield of the neutron probe being manufactured with synthetic

Table 2

Some characteristics of the four types of radiation

Name/Symbol	Mass	Charge	RBE*	Range
Alpha (α)	4	+2	20	2.5 cm in air (attenuation by one sheet of paper)
Beta (β)	0,0006	-1	1	Several cm in air (attenuation by 2.5 cm of wood)
Neutron (*n*)	1	0	5-10	30 m in air (attenuation by several cm of water)
Gamma (γ)	0	0	1	30 m in air (attenuation by several cm of lead)

*RBE = Relative Biological Efficacy = a relative index that quantifies the biological effect of the different types of radiation in the human body.

materials rich in hydrogen that are very efficient for neutron attenuation, the radiation

exposure dose rates for the operator are reduced and maintained at acceptable levels.

The gamma radiation has no charge and no mass. It is electromagnetic in nature moving at the speed of light in the form of photons. Differing only in their origin, gamma rays and X-rays have identical characteristics. Gamma rays originate from atomic nuclei while X-rays are emitted when electrons change their orbits around atomic nuclei. From a practical point of view, the great difficulty in the construction of efficient shields for portable gamma probes lies in the fact that the most efficient shield materials are heavy elements like lead (Pb).

2.2.2.4. Radiation Dose Rates for Neutron/Gamma Probes

Permissible levels of radiation dose rates for different occupational categories of the world's population have been derived from rules of international organizations for health and radiation protection. For persons who routinely handle radioactive sources during their work, the established level is 5 rem·y^{-1} or 5000 mrem·y^{-1}. Considering 50 working weeks per year, this value is about 100 mrem·week^{-1}. This dose rate is ten times higher than the average natural dose rate received by the population in general.

Most commercial neutron/gamma probes are built with the following radioactive sources, characteristics and dose rates, when outside of the shield:

Source	Activity	Dose Rate at 1 m from Source*
Cs-137	10m Ci	3.3 mrem·hr^{-1}
Am-241/Be	50m Ci	0.11 mrem·hr^{-1}
Both sources	60m Ci	3.41 mrem·hr^{-1}

*Dose rates for whole body reported in a CPN MC-3 Portaprobe Operating Manual

When the sources are inside shields (lead and carbide), the dose rate is reduced to 0.5 mrem·hr^{-1} at a distance of 1 m from the probe**. The largest exposure occurs during the manual transport of the equipment carried on the shoulders.** When carried by

its handle with arms extended, the dose rate is only about 0.5 mrem·hr^{-1}. For probes with neutron sources only, the dose rate is about 0.3 mrem·hr^{-1}.

When using a gamma/neutron probe, a worker is located in a radiation field of a given dose rate. To calculate the radiation dose rate received by the worker, multiply the dose rate by the exposure time.

Examples:

a) Handling of Neutron/Gamma Probes

Consider an average dose rate of 0.5 mrem·hr^{-1} equivalent to that of an operator carrying the probe by its handle with extended arms. What is the radiation dose rate received by an operator who makes twenty 3-min. measurements each day during a 5-d week?

Received radiation dose rate = 0.5 mrem·hr^{-1}(20 measurements)(0.05 hr·measurement^{-1})(5 d·week^{-1})

Received radiation dose rate = 2.5 mrem during 1 week

This dose is equivalent to 2.5% of the permissible weekly dose of 100 mrem.

b) Handling of Neutron Probes

Consider the dose rate to be 0.3 mrem·hr^{-1} for an operator working with the probe for a period of 5 hr every day for 5 d.

Received radiation dose rate = 0.3 mrem·hr^{-1}(5 hr·d^{-1})(5 d·week^{-1})

Received radiation dose rate = 7.5 mrem in one week

which corresponds to 7.5% of the permissible weekly dose of 100 mrem.

2.2.3. General Recommendations

A comprehensive presentation of the subject of radiation safety can be found in Chase and Chase & Rabinowitz (1967), Guzmán (1989) and other basic texts.

Although commercially available probes are designed and tested for ensuring operators to receive radiation exposure levels less than those permissible internationally, it is important to pay attention to the following aspects:

a) Personnel of low instruction level should not operate neutron probes, like any other radioactive material.

b) During their use, the operator should use a dosimeter for gamma radiation and neutrons.

c) Special care has to be taken in order to avoid exposure when the probe is outside of the shield. The handling of the source should be avoided and, when needed, should be done only by specialized personnel.

d) Any repair of probes should only be carried out by authorized personnel.

e) Probes should be stored in appropriate places for radioactive materials, far from places of circulation and permanence of people and animals, preferably key locked.

2.3. Access Tubes and their Installation

Size and type of access tubes depend on the diameter of the probe in use as well as the cost and availability of tubing. Unfortunately, because the diameter of probes has not been standardized internationally, manufacturers adopt tubing having a specific diameter for each kind of probe.

The best tubing material is aluminum because it is "transparent" to neutrons and does not generally corrode in most soils. When other materials are used (e.g. steel, iron and brass as well as polyethylene and other plastics), it must be recognized that these materials differ with respect to neutron interaction. Once a particular kind of tubing is chosen, calibration and all experimental work must be done with the same material. Steel and brass tubing affect slightly the sensitivity of probes owing to absorption of neutrons by iron and copper. Count rates are increased by the hydrogen in polyethylene and other plastic access tubes.

Each manufacturer normally specifies the inside and outside diameters of tubing. Because a large air gap between the probe and the wall of the tubing reduces the sensitivity of the measurement, the inside diameter of the tubing should be just large enough for the probe

to move freely without friction.

Tube length depends on the greatest depth to which measurements are made. Access tubes should always be 10 to 20 cm longer than the greatest measurement depth to allow the "active center" of the probe to be placed at the desired depth. Access tubes should also extend 20 to 40 cm above soil surface in order to facilitate the positioning of the probe shield case on top of the tube. Each access tube should be covered with rubber stopper or an inverted Aluminum can to avoid the entrance of water and debris. The bottom of each access tube should also to be sealed with a rubber stopper or other material to exclude water from a shallow water table. When the deepest measurements are above the water table, no stopper at the bottom of the tube is necessary.

Although there are several methods for installing access tubes (Greacen, 1981), each requires that a hole be made to the depth to which an access tube is placed into the soil. The primary purpose of each method is to avoid an air gap between the soil and the tube. This purpose is often achieved by using an auger with a slightly smaller diameter than the outside diameter of the access tube. After augering a hole to the desired depth, the access tube is driven with some difficulty into the hole while some soil cut from the wall of the hole enters the inside of the tube. The soil remaining inside the tube is removed with a second auger having a diameter slightly smaller than the inside diameter of the tube. Alternative methods consist of driving the tube directly into the soil in increments of about 20 cm. After each 20 cm increment, the soil inside the tube is removed with an auger slightly smaller than the inside diameter of the tube. Care must be taken to remove all of the soil inside the tube.

In some soils such as stony soils, heavy swelling soils and extremely layered soils, the installation of access tubes may be extremely difficult. In each case, the researcher has to use his own experience and ingenuity to properly install the access tubes. It should be remembered that the installation of an access tube is done only once for a given experiment and, therefore, it has to be done with much care, even if it takes great effort for several hours. An improperly installed access tube will compromise all measurements made in future. It should also be remembered that one of the great advantages of the neutron moderation method is the fact that the only disturbance made on the soil is during access tube installation and that, thereafter, quick measurements can be made over long periods, always "sampling" the same "point' in the field.

Repeating, it is essential make whatever effort is necessary to install in the best

possible way each access tube. More details about access tube installation can also be found in IAEA (1976).

2.4. Calibration

The calibration of a neutron probe consists in quantifying the relation between probe output cpm (counts·min^{-1}) and soil water content θ [(cm^3 of H_2O)·(cm^3 of bulk soil)$^{-1}$]. Samples of a given soil having a wide range in water content are used to measure cpm with the probe and θ in a classical manner. It is a simple procedure in theory but it might be difficult and tedious depending on the properties of the soil profile and the chosen experimental design. First, we discuss making a calibration curve for one depth of a homogeneous soil, and then extend our discussion to more difficult situations.

Sampling is the main problem in calibration. Theoretically, the same sample "exposed" to the neutron probe to obtain cpm should be used to measure θ. However, the neutron method "sees" a great volume, which is not well defined (assumed to be a sphere of 30 cm diameter), and classical soil moisture methods use samples many times smaller. This disparity is minimized by taking several soil samples for determining θ around the access tube near the position of the probe where cpm was obtained. In most cases, we are never guaranteed that both methods sampled the same volume of soil. The sampling problem becomes worse in heterogeneous, layered or stony soils.

Another practical problem is obtaining a wide range of water contents for the same soil. Although a wide range can be obtained by wetting (irrigation or rainfall) and drying (evaporation or drainage), it requires tedious operations for long periods of time over several locations. Because a soil does not wet or dry uniformly throughout its profile, the water content inferred by the neutron probe is a spatial average over an unknown volume of soil. Hence, both the position and volume of actual soil sampled remains somewhat ambiguous.

Having achieved the best set of data possible, we construct a calibration from pairs of data (cpm, θ) First, in order to avoid electronic drifts, temperature and other effects on the electronics of the neutron probe, we do not use cpm obtained in soil directly, but use the count ratio *CR* defined as:

$$CR = \frac{\text{count rate in soil}}{\text{count rate in standard}} = \frac{N}{N_s} = \frac{C \cdot T^{-1}}{C_s \cdot T_s^{-1}} \quad (5)$$

where C is number of counts measured in the soil during a period of time T (min), C_S number of counts measured in a standard material during a period of time T_S (min), N the count rate in the soil (cpm) and N_S the count rate in the standard material (cpm).

Table 3 shows field data obtained for the calibration of a probe for the 20 cm depth. Every time the neutron probe is used, it should be checked for stability by taking counting in a standard material. In most cases is taken with the probe inside its protection shield, positioned on the probe transportation case to maintain a standard condition. When water is used as a standard material, an access tube sealed at its bottom is placed in the center of a large container of water.

The standard count C_S gives us a standard count rate N_S that should be constant over long periods of time, fluctuating only within statistical deviations normally taken as $\pm C^{1/2}$ (Poisson's distribution). Each manufacturer gives details of these procedures for their probes.

Figure 2 shows the linear graph of θ versus CR. The solid line follows the equation (θ = -0.095 + 1.04CR) obtained through classical linear regression $\hat{y} = a + bx$. With CR taken as the independent variable and θ as the dependent variable, the linear regression coefficient is R = 0.966.

As will be shown later, the variance of the intercept a (-0.095) and that of the slope b (1.04), and their covariance contribute to the calibration error. Because these variances are the

Table 3
Calibration data for a probe with a source of 40 mCi Am/Be
Soil: Terra Roxa Estruturada (Alfisol) of Piracicaba, Brazil

Pairs	θ (cm3 cm-	N (cpm)	CR
1	0.424	79650	0.507
2	0.413	75541	0.481
3	0.393	76169	0.485
4	0.387	71143	0.453
5	0.378	67846	0.432
6	0.375	69259	0.441
7	0.306	59208	0.377
8	0.287	57637	0.367
9	0.291	62035	0.395
10	0.283	58109	0.370

N_s= count in water taken as standard = 157050 cpm

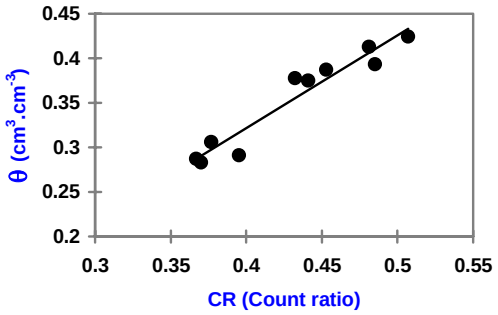

Figure 2 – Calibration equation obtained with Table 3 data.

primary errors in the use of neutron probes, their magnitudes must be minimized. In general, the closer the value of *R* is to unity, the smaller are these variances. Provided the data are indeed linear, values of *R* close to unity can be achieved by increasing the number of pairs of observations (cpm, θ) and increase the range of soil water content measured, taking very wet (close to or at saturation) and very dry points.

The intercept of a calibration curve varies from soil to soil and from probe to probe. It has not to be zero or close to zero, since it is an extrapolated value, out of the calibration range. Although there is no strong theoretical meaning given to the intercept, it is nevertheless related to the residual H content of the soil.

The slope of the calibration also varies from soil to soil and from probe to probe. Being the derivative of the calibration line, it represents the sensitivity of the probe. It is the change in soil water content per unit change in count ratio. Within certain limits, the smaller is its value, the more sensitive is the probe. In other words, for small changes in soil water content (the variable we desire), we have great changes in count ratio (the variable we measure).

Because of the processes of neutron interaction in the soil, geometry of the probe, type of neutron detector, electronics, etc, each soil has a specific calibration line for a given neutron probe. Soil characteristics (mainly chemical composition and bulk density) also affect the calibration line. Therefore, for a specific soil, calibration lines are related to different soil bulk densities ρ_b (Figure 3). In general, the calibration lines for different bulk densities of the same soil are parallel, having the same slope. For extremely layered soils, especially those

with layers of different composition like some alluvial soils, the slopes differ for each layer.

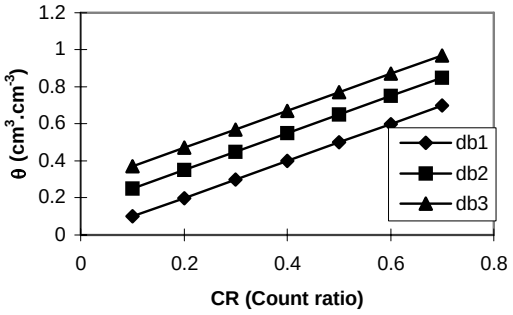

Figure 3 – Schematic examples of calibration equations for different soil bulk densities $\rho_{b1} > \rho_{b2} > \rho_{b3}$

In addition to the difficulty of installing access tubes, stony or gravely soils are a special problem. The definition of θ is also difficult; Some authors define θ using the bulk volume for the total sample volume including the volume occupied by gravel, while others exclude the volume occupied by gravel. With each gravelly soil being a different case, the neutron probe user will have to explore the best means of obtaining useful calibration curves. The necessity of different calibration curves for slightly different soils or for slightly different bulk densities will depend on the objectives of each experiment. The accuracy needed for the determination of θ will be the most important criterion for judgement.

2.4.1. Laboratory Calibration

Laboratory calibration involves the use of packed soil samples with discrete levels of soil water content θ and soil bulk density ρ_b. Usually, great amounts of soil are packed into drums of 80 to 120 cm diameter and 80 to 120 cm height. An access tube is placed in the center of the drum. Packing should be done carefully in order to obtain a homogeneous distributions of θ and ρ_b throughout the sample. Obtaining uniform distributions is a very difficult, laborious task.

Many neutron probe manufacturers have a collection of such sealed drums

representing a wide range in soil water content in order to calibrate each new probe. The calibration data obtained from such drums is called the factory calibration curve. Although its use is somewhat limited because it is derived for only one soil or soil material, it is useful to compare the factory calibration to that for a soil being studied by a user. Commonly, because their slopes are nearly identical, the factory calibration curve can be used when the interest is only measuring changes in soil water content, not absolute values of θ.

2.4.2. Field Calibration

Field calibration involves the installation of access tubes directly into a field soil with measurements of cpm being made with the probe and soil samples collected immediately at the same depths around the access tube to measure θ by any classical method. This procedure is repeated using several access tubes at a given time to obtain a desired number of replicated sets of observations of θ and cpm within a soil profile for a given distribution of soil water content. At other times, when soil water contents vary from very wet to very dry, the procedure is repeated again and again with more access tube locations to achieve paired observations of θ and cpm over the entire range of potential soil water contents to be later monitored in field investigations. Under normal field conditions it is difficult to find such a wide range of soil moisture. To obtain very wet conditions, irrigation is recommended. Dry conditions are more difficult to obtain especially in humid and subhumid regions. And in arid regions even with water being extracted by plant roots, the soil water content does not decrease much below the permanent wilting percentage except near the soil surface owing to evaporation. Because soils do not dry at the same rate at every depth as well as being stratified, the resulting non-uniform distribution of θ within their profiles introduces error in the calibration of neutron probes.

2.4.3. Quick Field Calibration

Carneiro and De Jong (1985) presented a method for quickly obtaining a calibration curve in the field. The method consists of using a neutron probe to measure the change in count ratio within the soil profile as a result of applying a known amount of irrigation water.

The slope *b* of the calibration is determined from the equation:

$$b = \frac{S_f - S_i}{[\sum_0^z CR_f \cdot \Delta z - \sum_0^z CR_i \cdot \Delta z]} \quad (6)$$

where S_f is the final soil water storage calculated from soil surface down to the water penetration depth *z*, S_i the initial soil water storage to depth *z* and CR_f and CR_i the final count rates corresponding to depth increases Δz, respectively. Because the change in soil water storage corresponds to the applied irrigation water depth, the difference (S_f - S_i) is known, and hence *b* of the neutron calibration curve is known. The value of *a* is calculated from:

$$a = \theta - bCR \quad (7)$$

with the value of θ obtained from a soil sample taken from the field at the time *CR* was measured with the neutron probe. The soil sample is analyzed gravimetrically in the laboratory.

Example: Before and after the application of 150 mm (15 cm) of water to a soil, the following count rates were obtained at different depths:

Depth (cm)	CR_i	$CR_i \cdot \Delta z$	CR_f	$CR_f \cdot \Delta z$
0-30	0.22	6.6	0.55	16.5
30-60	0.35	10.5	0.58	17.4
60-90	0.32	9.6	0.40	12.0
90-120	0.30	9.0	0.30	9.0
	$\sum_0^{120} CR_i \cdot \Delta z$	35.7	$\sum_0^{120} CR_f \cdot \Delta z$	54.9

The slope of the calibration curve is calculated as:

$$b = \frac{S_f - S_i}{[\sum_0^z CR_f \cdot \Delta z - \sum_0^z CR_i \cdot \Delta z]} = \frac{15}{54.9 - 35.7} = 0.781$$

A soil sample taken in another situation at the 30 cm depth had a gravimetric soil water content θ = 0.434 $cm^3 \cdot cm^{-3}$. The corresponding *CR* obtained in the field at the same depth was 0.45. Therefore, with the value of *a* calculated as

$$a = \theta - bCR = 0.434 - 0.781(0.45) = 0.0824$$

the final calibration equation becomes

$$\theta = 0.0824 + 0.781CR$$

2.4.4. Theoretical Models

Calibration equations have also been developed from theoretical models based on neutron diffusion theory. One of the most accepted models (Couchat et al., 1975) is based on the measurement of neutron absorption and diffusion cross sections in a graphite pile. Soil samples analyzed in a specialized laboratory having a graphite pile yield a linear calibration equation as a function of soil moisture and bulk density. Vachaud et al. (1977) presents a systematic study of comparison between gravimetric and theoretical calibrations.

2.4.5. Calibration for Surface Layers

The calibration of neutron probes for measuring the soil water content near the soil surface requires a special effort. Many people recommend not using depth neutron probes near the soil surface, but use any other classical method. There are surface neutron probes, as shown in Figure 7 (chapter 3), which are specially designed for surface measurements.

Several approaches have been used for measuring soil water in surface soils. One approach which takes into account the escape of neutrons to the atmosphere (Greacen, 1981) is to obtain separate calibration curves for each individual shallow depth layer. Another is to use neutron deflector/absorbers made of paraffin or polyethylene. A hole in the center of thick

discs of paraffin or polyethylene allow these deflector/absorbers to be placed on top of soil surface immediately around the access tube (Arslan et al., 1997). Although this approach provides reliable calibration curves, the use of these deflector/absorbers for routine measurements has proven unpractical in many situations.

2.5. Sphere of Influence

The probe "sees" an approximately spherical cloud of slow neutrons formed immediately after it is placed at a desired soil depth. This sphere is called "sphere of influence" or "sphere of importance" of the probe. Theoretical studies (IAEA, 1970) show that its radius is a function of the soil water content (hydrogen content). In pure water, the radius of the sphere of influence is in the order of 5 to 8 cm. In very dry soils, this radius may increase to 20 cm or more. Olgaard's (1969) theoretical model suggests that for a value of θ = 0.1 $cm^3 \cdot cm^{-3}$ which is extremely low for agronomic purposes, the radius is always less than 45 cm. Because this sphere of influence is not constant even for the same soil using the same probe, special consideration should be given to the measurement and interpretation of neutron probe readings both in the field as well as when making a calibration curve. This consideration is particularly important for shallow depths in dry soils. By knowing the radius of the sphere of influence as a function of θ, the probe can be placed just deep enough into the soil profile to prevent the loss of neutrons to the atmosphere.

It is best to measure the radius of the sphere of influence in the laboratory using homogeneous soil uniformly packed soil in drums. Measurements can also be done in the field whenever water content distributions are nearly constant within a fairly homogeneous soil. The experimental procedure is very simple. The probe is lowered to a depth greater than the radius of influence R_i. Because R_i is not known initially, and is usually less than 45 cm, we lower the probe to the 50 cm depth. After taking an initial count rate at 50 cm, the probe is raised sequentially in small increments through the soil surface to a few positions above the soil surface. Ideally, the depth intervals should be 1 cm, but should never exceed 5 cm. When the probe is at 50 cm or greater depths, neutrons should not escape to the atmosphere, and count rates should be fairly constant, fluctuating only within the statistically permissible limits of $\pm\sqrt{C}$. As the active center of the probe approaches the soil surface, some neutrons escape

to the atmosphere and the count rate decreases proportionately. As the probe continues to pass through the soil surface and into the atmosphere, the count rate exponentially decreases to very low values. See Table 4 and Figure 4. **(Owing to this escape of fast neutrons the operator should take care of his protection, standing as far as possible from the probe.)** From the graph of the count rate as a function of depth, the value of R_i is the depth where the count rate starts to decrease.

Table 4

Count rate (cpm) as a function of depth for two homogeneous media: water and soil at θ = 0.35 $cm^3 \cdot cm^{-3}$

Depth (cm)	N	N
100	157230	67100
90	157110	67030
80	157130	66880
70	157020	66950
60	156890	67230
50	157150	67310
40	156970	68910
30	157080	68370
20	157160	67250
15	157020	68630
12.5	157240	66870
10	157000	64150
7.5	156540	59800
5	145230	54360
2.5	125810	42550
0	75440	29120
-5 (in air)	30770	26670
-10 (in air)	15300	14590
-20 (in air)	5110	5670

Falleiros (1994) has recently extended the above methodology for heterogeneous soils or soils with heterogeneous water contents. By using two sets of measurements – one with and one without the use of neutron deflector/absorbers, he was able to easily define the radius of influence.

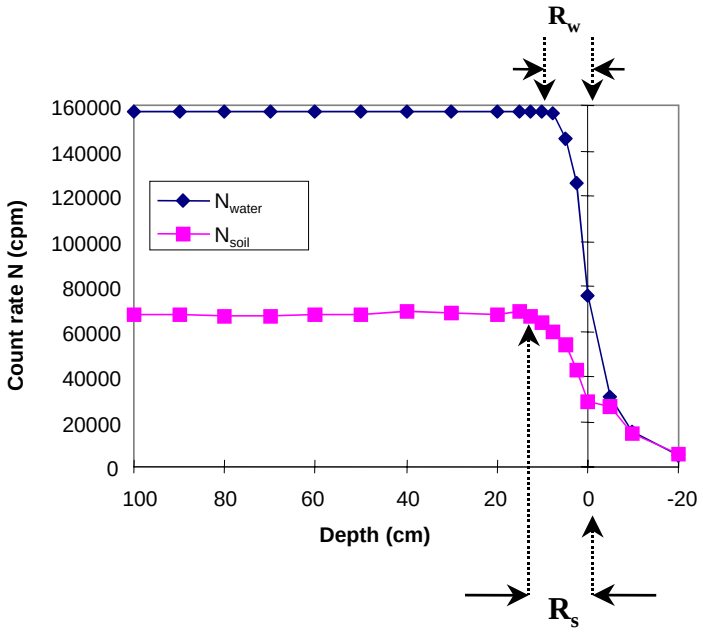

Figure 4 – Spheres of influence in soil and water.

3. Neutron/Gamma Probe for Simultaneous Measurement of Soil Bulk Density and Water content

3.1. General Characteristics

In addition to the depth neutron probes described in Chapter 2, there are probes that allow the simultaneous measurement of soil bulk density and water content. For this purpose, they have a fast neutron source (often $^{241}Am + {}^{9}Be$) with a slow neutron detector (^{3}He chamber), and a gamma ray source (often ^{137}Cs) with a Geiger-Mueller type detector . Depth probes and surface probes are available. Depth probes require the installation of access tubes in the soil profile. Surface probes measure the average soil water content of the surface layer (0 – 15 cm) and the bulk density of various layers having a thickness of 2.5 to 30 cm depending on the probe model. Except for the fact that the fast neutron source and slow neutron detector are fixed to the base of the shield not allowing measurements at various soil depths, soil water content measurements and calibration procedures for the surface probes are identical to those described in Chapter 2. With respect to bulk density measurements, depth

probes are based on the back-scattering of gamma radiation, while surface probes rely on both back-scattering and attenuation of gamma radiation.

In this chapter we focus only on surface probes used to measure soil bulk density by back-scattering as well as by attenuation. With slight modifications, the aspects treated here can easily be adapted for depth neutron/gamma probes.

Figures 7a and 7b show a surface neutron/gamma probe being used with its gamma source in two modes of operation. In mode (a), the gamma source is not lowered into the soil and can occupy two positions: BS, a little above soil surface, and AC at the soil surface. Measurements in both positions are made by back-scattering only and the soil bulk density evaluation is made on the soil surface layer. In mode (b), the gamma source is lowered into the soil to the desired depth (from 5 to 30 cm in 2.5 cm intervals) and the bulk density is measured by both processes, gamma-ray back-scattering and gamma-ray attenuation. For both modes of operation (a) and (b), the average soil water content of the soil surface (0 – 15 cm) is measured by neutron moderation, using a neutron source fixed at the soil surface.

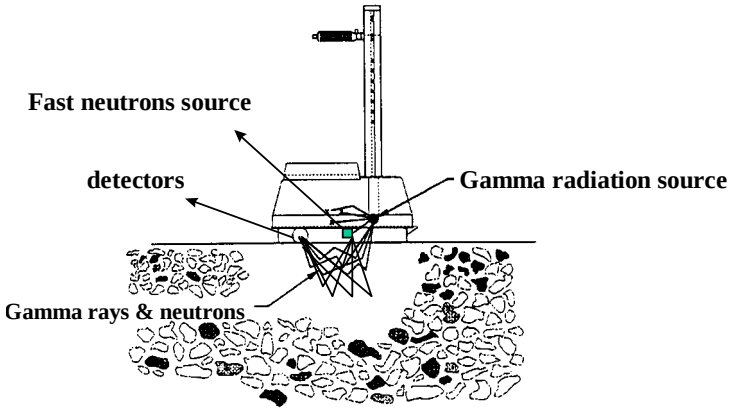

Figure 7a – Probe in position to measure soil water content and bulk density of the surface layer, by back-scattering only. *Source: CPN MC-3 Portaprobe Operating Manual*

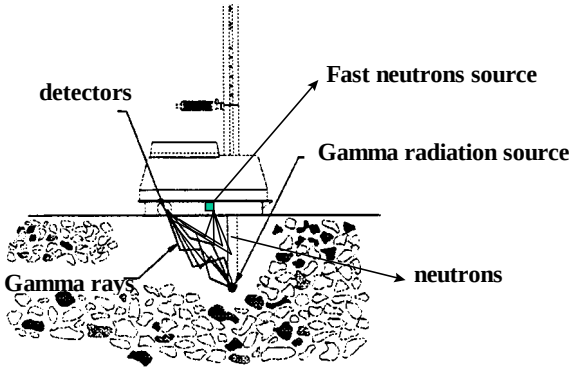

Figure 7b – Probe in position to measure soil water content of the surface layer and soil bulk density from soil surface down to desired depth, by attenuation and back-scattering. *Source: CPN MC-3 Portaprobe Operating Manual*

In these probes, the fast neutron source is fixed to the base of the shield in such a way that when in contact with the soil, the source is located at the probe/soil interface. The gamma-ray source is located at the tip of a movable stainless steel rod which permits its introduction into the soil down to the desired depth through a hole previously made with a small auger furnished by the manufacturer. Both gamma-ray and slow neutron detectors (Geiger-Mueller and Helium-3) remain together at a fixed position at the base of the shield near the probe/soil interface when the probe is on the soil.

3.2. Working Principle

With respect to the soil water content measurement, the surface neutron/gamma probes work according to the same principle of the depth probes discussed in Chapter 2, considering only half sphere of influence that covers the first 15cm depth, approximately. As already mentioned, for the measurement of soil bulk density, the surface probes use two different physical processes: a) gamma-radiation back-scattering and b) gamma-ray attenuation.

a) Back-scattering

For surface measurements of the bulk density of soil and other materials such as concrete or asphalt paving, as shown in Figure 7a, the gamma-ray detector measures the number of photons that return to the soil surface after interacting (backscattering) with atoms of soil particles. The number of back-scattered photons is related to the density of the medium, and follows the model of the Figure 8.

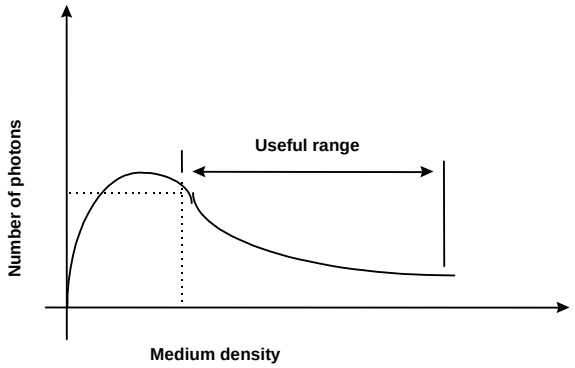

Figure 8 – Effect of medium density on the number of "reflected" photons.

The useful range of this relation used for the measurement of soil bulk density is shown in the figure 8. In this range, the relation between medium bulk density ρ'_b and the backscattered photon count ratio *CR* follows the model according to:

$$\rho_b^{'} = B \ln\left(\frac{A}{CR - C}\right) \tag{61}$$

where *A*, *B* and *C* are parameters determined experimentally using materials of known density as indicated in Table 14 and Figure 9 and CR is the count ratio (backscattered photon count in the soil/standard density count)

If the soil is moist during the measurement, part of the measured back-scattered radiation is caused by soil water. The dry soil bulk density ρ_b is related to the wet soil bulk density ρ'_b by the relation

$$\rho_b = \rho_b^{'} - \rho_w \theta \tag{62}$$

where ρ_w is the water specific weight. For practical purposes, taking ρ_w = 1g·cm^{-3}, we have

$$\rho_b = \rho_b^{'} - \theta . \tag{63}$$

Inasmuch as the probe simultaneously measures θ through neutron moderation, the value of the dry bulk density is readily available.

b) Attenuation

In the depth measurements as indicated in Figure 7b, the gamma-ray detector counts both the number of photons that cross the soil sample of thickness *X* located in the direction between the gamma-ray source and the detector, and the number of back-scattered gamma rays. Therefore only part of the photons that reaches the detector, after crossing the soil thickness X, can be associated to the Beer-Lambert's law of attenuation, according to equation 64.

$$I = I_0 \exp\left[-(\mu_w \theta + \mu_s \rho_b)X\right] \tag{64}$$

where *I* is the number of photons that reach the detector per unit of time after passing through a soil sample of thickness *X*, I_0 is the number of photons that reach the detector per unit of time in the absence of soil for the same distance *X* between source and detector; μ_W and μ_S are the attenuation coefficients of the gamma-rays by water and soil, respectively, being specific for the energy of the gamma-rays of the source used, ρ_S the soil bulk density and θ the water content. Since only part of the interactions is described by equation (64), calibration curves for such neutron/gamma probes are established experimentally using the same model presented above for back-scattering. In this case, the count ratio CR includes the back-scattered and the transmitted photons. The parameters *A*, *B* and *C* are obtained from

measurements in materials of known thickness and density as shown in Table 11 and Figure 9.

Similar to the measurement of bulk density of a moist soil by back-scattering, part of the photons not counted by the detector are due to the attenuation by the soil water. From these measured values of wet bulk density the dry soil bulk density can be obtained using equation (63).

3.3. Calibration

Due to the relative complexity of their calibration, most neutron/gamma probes have factory calibrations that are already stored in the memory of their microprocessor. Their calibrations for density determination are complex because a) they require the use of standardized blocks of special materials of different densities, and b) the parameters of the mathematical model are difficult to obtain. Only when appropriate facilities are available can these factory calibrations be modified or recalculated by the user. Some models of probes with mathematical processors allow calibration if a set of standard blocks is available for the user. For such a calibration, blocks having at least three different densities (low, medium and high) and two different equivalent water contents [1](low and high) are required. It is also sometimes possible to modify the values of the parameters in the calibration equations stored in the probe microprocessor to obtain a better relation between the readings and measured values.

Some probes provide an opportunity to store correction coefficients for automatically adjusting their calibration for specific soil conditions. For example, soil water content is overestimated with a probe in soils having high organic matter content, high content of calcareous materials or hydrogen sources other than water. For automatic corrections of water contents in such soils, the deviation from the probe reading in relation to the real value measured in the laboratory by gravimetry is introduced into the memory of the processor. This kind of correction can be used to adjust the factory calibration regardless of the cause of the observed systematic differences. It is also possible to substitute totally the equation furnished by the manufacturer for water content without causing changes in the equations for density, as it was recommended previously for the depth probes.

---

[1] *Equivalent water content refers to materials of known hydrogen content, equivalent to a given water content, for reasons of neutron moderation.*

Table 14 shows the contents of the memory in a microprocessor of a surface neutron/gamma probe related to its calibration for density.

The memory data refer to: a) counting of photons (gamma-rays) for the different depths of the gamma source in three different standard media of known density; b) standard counting for density (photon counting in the standard position over a standard block that belongs to the equipment); c) values of the coefficients *A*, *B* and *C* of the calibration equations [eq.(61)] for the different depths; d) date of the standard counting and e) date of calibration. Figure 9 shows the calibration curves of the probe when operating at positions BS and AC (table 14) which allow density measurements of thin surface layers when drilling a hole for the introduction of the rod is not feasible. In both BS and AC positions, the probe uses the

Table 14 – Microprocessor memory contents of a probe CPN model MC-3 with respect to density calibration.

Standard Density Count: 37426						
Date of Calibration: 23/09/1996						
Counting in:				Equation Parameters		
Depth	1.717 $g.cm^{-3}$	2.14 $g.cm^{-3}$	2.632 $g.cm^{-3}$	*A*	*B*	*C*
BS	27159	20136	14882	2.96370	1.03103	0.16876
AC	54791	40970	29425	4.88411	1.37661	0.06809
5	137842	102072	70641	12.05662	1.62628	-0.49339
7.5	136354	98474	65574	12.87482	1.56126	-0.62528
10.0	127121	88344	57156	14.42408	1.23470	-0.17691
12.5	113500	75368	46739	15.98036	1.03949	-0.01576
15.0	97338	62090	36633	15.98228	0.95437	-0.03037
17.5	80888	49047	27488	16.69699	0.83982	0.01083
20.0	65356	37486	20262	18.38896	0.71770	0.07412
22.5	51567	28224	14730	18.47506	0.64857	0.07612
22.5	51567	28224	14730	18.47506	0.64857	0.07612
25.0	40144	21170	10764	17.44628	0.60277	0.06743
27.5	30940	15776	8083	17.57011	0.54558	0.07583
30.0	23728	11953	6165	14.97285	0.52603	0.06478

back-scattering principle. At the raised BS position the source is maintained slightly above soil surface, so that gamma-rays penetrate into the medium at a small solid angle. Therefore, the probe evaluates the average density of a little thicker layer than at position AC, in which the source is maintained at soil surface and gamma-rays penetrate into the medium in a solid angle of 2π sphero-radians. The effect of soil surface roughness is the minimized at position BS. At position AC the gamma source is in the plane of the soil surface, and the probe evaluates the average density of a thinner layer, close to surface.

Figure 10 shows the attenuation calibration for operation positions corresponding to depths ranging from 5 to 30 cm. In this case the value of the density corresponds to the soil sample crossed by the gamma beam, that is, between source and detector, and both phenomena, back-scattering and attenuation play a role in the measurements.

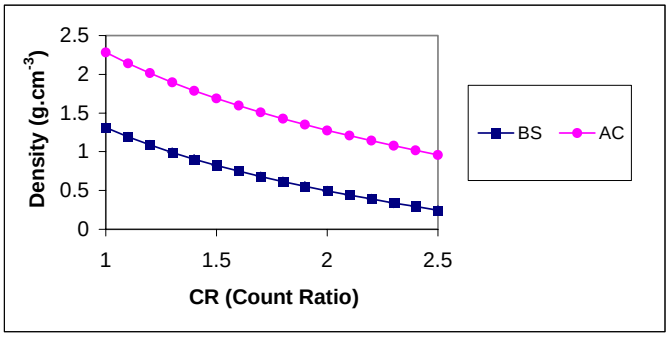

Figure 9 – Calibration curves of a probe for the measurement of the density of a porous medium utilizing the process of gamma-ray back-scattering.

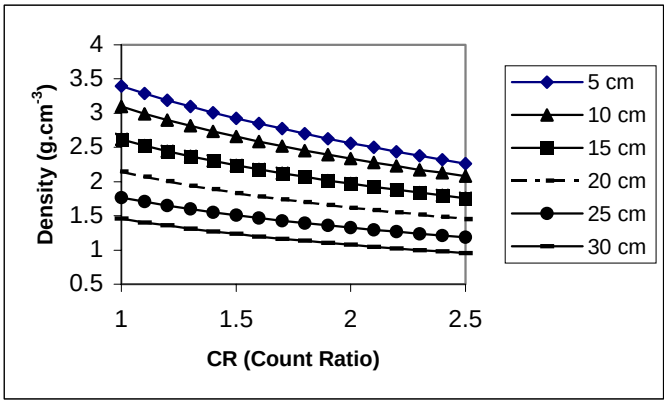

Figure 10 – Calibration curves of a probe for the measurement of the density of a porous medium utilizing both processes of gamma-ray attenuation and back-scattering through

different soil thickness.

Table 15 shows the contents of the memory of a microprocessor of a surface neutron/gamma probe in relation to its calibration for water content measurements. The stored data refer to: a) standard counting for water content (counting of slow neutrons at the standard position over a standard block that belongs to the equipment); b) date of the standard counting; c) date of calibration; d) counting of slow neutrons for standard blocks with known equivalent water contents and e) values of the coefficients *A* and *B* of the calibration equation for water content. As is the case for all other depth neutron probes, the calibration is the linear model:

$$\theta = A + B \cdot CR \tag{65}$$

where θ is the volumetric soil water content t ($cm^3 \cdot cm^{-3}$) and *CR* the relative count rate.

Table 15

Contents of the memory of the microprocessor of a CPN probe, model MC-3, with respect to the calibration for soil water content.

Standard Counting for Water Content: 83344; Date: 23/09/1996			
Date of Calibration: 23/09/1996			
Counting for		Equation Coefficients	
$\theta = 0$ $cm^3 \cdot cm^{-3}$	$\theta = 0.53$ $cm^3 \cdot cm^{-3}$	*A*	*B*
337	5263	-0.03627	0.90265

4. APPLICATIONS

4.1. Soil Water Storage

Although this subject has already been discussed in item 2.6.3, we will now give an example of a practical application. The water stored in a soil layer between depths L_1 and L_2 at time *t* is defined as:

$$S_{L_2-L_1}(t) = \int_{L_1}^{L_2} \theta(z,t)dz \quad (66)$$

where θ is the volumetric soil water content given by equation (2) and z is the vertical position coordinate, measured downwards from soil surface. Using θ in units cm^3 of water per cm^3 of soil, and z in cm, S becomes equivalent to a height of water measured in cm. Each cm of stored water corresponds to a volume of 10 liters of water per square meter of soil surface from the soil surface down to the integrated depth. The most common case is when $L_1 = 0$ (soil surface) and the integration is made over the entire soil profile to depth L_2.

As already discussed, because a general function $\theta(z)$ describing the variation of θ along z is not known, it is necessary to use numerical schemes of integration as presented earlier. Because the trapezoidal rule is entirely adequate for most agronomic purposes, we shall not present other integration schemes.

According to the trapezoidal rule, equation (37) is simplified to:

$$S_{L_2-L_1}(t) = \bar{\theta}(L_2 - L_1) \quad (67)$$

where $\bar{\theta}$ is the average value of θ in the interval (L_1 - L_2). Table 16 shows water content data collected in an access tube installed in a corn field.

Table 16

Count ratios and soil water contents as a function of soil depth for a corn crop growing on an Alfisol

Depth (cm)	Count Ratio (CR)	Soil Water Content ($cm^3 \cdot cm^{-3}$)
25	0.494	0.420
50	0.485	0.410
75	0.503	0.429
100	0.473	0.398
125	0.465	0.389
150	0.471	0.396

Using equation (67), the following soil water storage are calculated with little difficulty:

$$S_{150 - 0} = 0.407\ (150 - 0) = 61.1\ \text{cm}$$

$$S_{75 - 0} = 0.420\ (75 - 0) = 31.5\ \text{cm}$$

$$S_{100 - 50} = 0.412\ (100 - 50) = 20.6\ \text{cm}$$

It is important to know the "sphere of influence" of the probe especially for measurements close to soil surface. In the present example, the "sphere of influence" has a radius of order 15 cm. This means that when the probe is placed at the 25 cm depth, we are making a measurement across the 10- to 40 cm depth. Because we are not measuring the water content in the top 10 cm of soil, our soil water storage calculations near the soil surface are not necessarily accurate. On the other hand, because we are sure that neutrons did not escape from soil surface, our measurement at the 25 cm depth is accurate. Hence, it is advantageous to take gravimetric samples at the soil surface.

It is also important to remember that a neutron probe averages the distribution of water over a soil layer having a thickness of the diameter of the sphere of influence. Figure 11 illustrates this averaging for the data of Table 16. The shaded areas illustrate where the spheres of influence overlap. It is altogether appropriate that the probe measures an average water content because, indeed, the calculations made with equation (67) are based on average values. Even when probe measurements are taken close to each other with their spheres of influence overlapping, no harm is done – on the contrary, it improves the sampling of the total amount of water in the profile.

In this example, had measurements been taken at 10 cm depth intervals, the overlapping would have resulted in a better estimate of water stored in the 150 cm soil profile. For such a sampling program however, we would have had to pay attention near the soil surface where a measurement at 10 cm would have resulted in part of the sphere of influence being outside the topsoil.

Modern models of neutron probes have microprocessors that calculate automatically the soil water storage, giving results in mm of water or other appropriate units. Others, still

more sophisticated, move up and down in the access tube at a constant speed, making an excellent integration of the soil water distribution and providing a single count rate representing an integrated value of the amount of water in the profile.

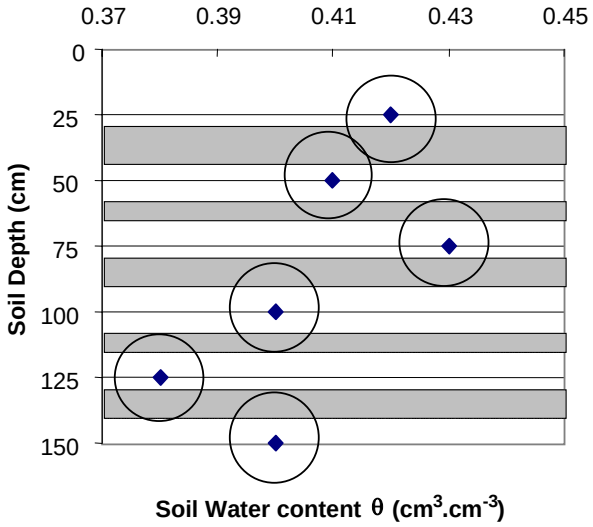

Figure 11 – Soil water content profile measured in an Alfisol cropped to corn in Piracicaba, Brazil

Another important aspect is the monitoring of soil water content changes in time. As soil gains water by rainfall or irrigation, or as it loses water by evapo-transpiration or internal drainage, soil water storage changes as a function of time.

Example: For the same corn crop, neutron probe measurements made at different dates gave the following storages:

S_{150-0}(07/09/98) = 611.0 mm

S_{150-0}(14/09/98) = 579.5 mm

S_{150-0}(21/09/98) = 543.8 mm

S_{150-0}(28/09/98) = 575.8 mm

From 7 to 21/09 there was no rain or irrigation. The average rates of water loss were:

$$\frac{\partial S}{\partial t} \approx \frac{S_{150-0}(14/9) - S_{150-0}(7/9)}{14-7} = -4.5\,\mathrm{mm \cdot d^{-1}}$$

$$\frac{\partial S}{\partial t} \approx \frac{S_{150-0}(21/9) - S_{150-0}(14/9)}{21-14} = -5.1\,\mathrm{mm \cdot d^{-1}}$$

These losses potentially occur as evapo-transpiration, and drainage below the 150 cm soil depth. With only these data, we are unable to partition the evapo-transpiration loss from that of drainage. Rain occurred during the period 21 to 28/09, and hence soil water storage increased with an average rate of:

$$\frac{\partial S}{\partial t} \approx \frac{S_{150-0}(28/9) - S_{150-0}(21/9)}{28-21} = 4.57\,\mathrm{mm \cdot d^{-1}}$$

This increase is the net result of rainfall exceeding the combined losses from runoff, evapo-transpiration, and drainage below the 150 cm soil depth.

4.2. Field soil water retention curves

Field soil water retention curves are established by combining neutron probe readings with those of tensiometers taken at the same time for the same soil depth. Tensiometers should be installed close to neutron access tubes just outside the "sphere of influence" of the probe. If tensiometers are installed too close to the access tubes, the water inside the tensiometer cup interferes significantly with proper functioning of the probe. A distance of 20 to 30 cm is adequate to avoid the interference.

The physical properties of field soils are known to be spatially variable even over relatively small distances. Owing to spatial variability of their field soils, Greminger et al. (1985) and Villagra et al. (1988) had difficulty ascertaining accurate and precise soil water retention curves. IAEA (1984) also presents soil water retention curves obtained with tensiometers and neutron probes for soils of several countries. Figures 12 and 13 are two examples of soil water retention curves obtained from neutron probe and tensiometer data.

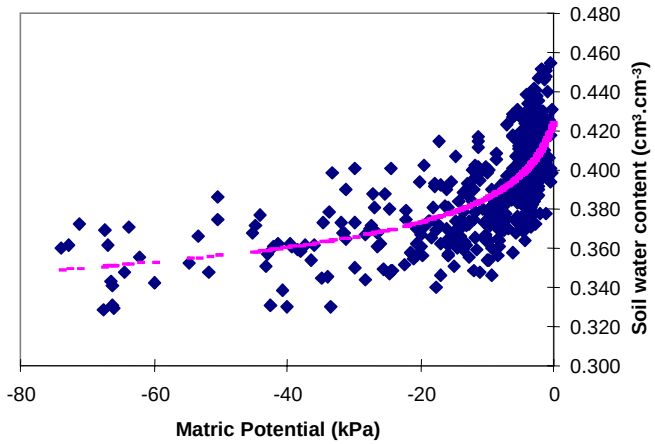

Figure 12 – Soil water retention curve for an Alfisol measured at the 20 cm (Villagra et al. 1988)

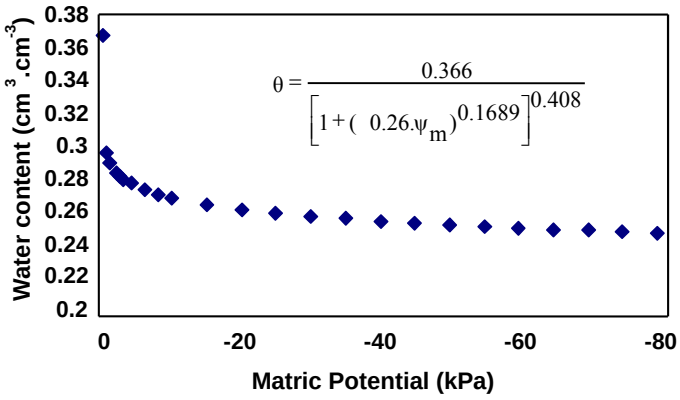

Figure 13 – Average soil water retention curve measured in field soils of several countries (IAEA, 1984)

4.3. Soil hydraulic conductivity

Soil hydraulic conductivity K is a parameter that indicates the ability of a soil to transmit water. Because it is strongly dependent on soil water content θ, we define the function $K(\theta)$ for each soil. Hence, all methods used to measure hydraulic conductivity require the measurement of soil water content. Among the methods developed for field

conditions, the use of a neutron probe is especially convenient and appropriate. As examples, we illustrate here the methods presented by Richards et al. (1956), Libardi et al. (1980) and Sisson et al. (1980).

To determine the $K(\theta)$ function, neutron access tubes and tensiometers are installed down to the desired depths in a level field plot having an area of at least 9 m^2 and generally less than 100m^2. Water is continuously ponded on its surface to a minimum water depth until infiltration reaches an approximate steady state condition. This condition is also signaled by neutron probe readings remaining constant with time and soil water contents approaching maximum relative values at each depth within the profile. The steady state infiltration rate into the soil surface is recorded and assumed equal to the hydraulic conductivity K_0 of the topsoil corresponding to the soil water content θ_0 of the topsoil during the time of steady infiltration. The most commonly used function of $K(\theta)$ is

$$K(\theta) = K_0 \exp[\gamma(\theta - \theta_0)] \qquad (68)$$

where the value of γ is determined from measurements taken after infiltration and during the time water redistributes and drains from the soil in the absence of plant roots and evaporation.

After infiltration when water is no longer applied to the plot and the ponded water disappears into the soil surface, the soil is covered with plastic to prevent evaporation, and periodic measurements of soil water content and soil water matric potential are taken at the selected depths with a neutron probe and tensiometers, respectively. Considering that the soil water redistribution process begins at $t = 0$ (the moment that water is no longer ponded on the plot), measurements of soil water content $\theta(z, t)$ such as those given in Table 17 are obtained. Simultaneous measurements of soil water matric potential $\psi_m(z, t)$ are added to the gravitational potential z to obtain values of the total soil water potential $\psi_T(z, t) = (\psi_m(z, t) + z)$ such as those given in Table 18.

The value of the hydraulic conductivity K_0 measured during steady state infiltration was 2.2 $cm \cdot d^{-1}$. This value together with those of $\theta(z, t)$ and $\psi_T(z, t)$ presented in Tables 17 and 18, respectively, will be used in calculations of $K(\theta)$ using the following three methods.

Table 17

Soil water contents during redistribution

Depth	Soil Water Content θ ($cm^3 \cdot cm^{-3}$)				
(cm)	$t = 0$	$t = 1$ d	$t = 3$ d	$t = 7$ d	$t = 15$ d
0	0.500	0.463	0.433	0.413	0.396
30	0.501	0.466	0.432	0.414	0.398
60	0.458	0.405	0.375	0.347	0.307
90	0.475	0.453	0.438	0.423	0.414
120	0.486	0.464	0.452	0.440	0.427

Table 18

Total soil water potential head during redistribution

Depth	Total Soil Water Potential Head ψ_T (cm)				
(cm)	$t = 0$	$t = 1$ d	$t = 3$ d	$t = 7$ d	$t = 15$ d
15	-18	-38	-69	-100	-135
45	-47	-76	-104	-129	-164
75	-76	-105	-135	-163	-200
105	-108	-141	-172	-206	-229
135	-140	-172	-201	-240	-265

4.3.1. Richards et al. (1956) Method

This drainage-flux method, initiated by Richards et al. (1956), was developed further by Nielsen et al. (1964), Rose et al. (1965) and van Bavel et al. (1968). It is now recognized as the instantaneous profile method (Watson, 1966). Since then, the method has been used by many other investigators to determine the hydraulic conductivity of well-drained soils. The method assumes that the rate of decrease of water stored in a profile for $0 \leq z \leq L$ during redistribution in the absence of evaporation and water absorption by plant roots is equal to the soil water flux density at depth L. Hence,

$$K[\theta(L)] = \left[\int_0^L \frac{\partial\theta(z,t)}{\partial t}dz\right]\cdot\left(\frac{\partial\psi_T}{\partial z}\right)^{-1} = \frac{\partial S(L,t)}{\partial t}\cdot\left(\frac{\partial\psi_T}{\partial z}\right)^{-1} \qquad (69)$$

where the integral is the soil water flux density and the gradient of the total soil water potential head is measured at $z = L$. The integral is evaluated by first calculating the water stored $S(L, t)$ using equation (67) for each measurement time. The derivative of $S(L, t)$ can be approximated using the difference method for a given time period. Or, the values of $S(L, t)$ from equation (67) can be used in a regression equation of the form $S(L,t) = a + b\ln t$, and subsequently taking the time derivative to obtain $b \cdot t^{-1}$, the soil water flux density at any time t. For that time, the total soil water potential gradient can be approximated using the difference method for a given depth interval.

Example:

The soil water content data in Table 17 are converted to soil water storage $S(L, t)$ using equation (67) for values of L = 30, 60, 90 and 120 cm.

Depth L	Soil Water Storage $S(L, t)$ (mm)				
(cm)	t = 0	t = 1 d	t = 3 d	t = 7 d	t = 15 d
30	150.1	139.4	129.5	124.1	119.1
60	291.8	266.8	248.0	234.8	220.2
90	435.2	402.8	377.6	359.3	340.9
120	580.8	540.2	511.2	488.9	466.1

With these data of $S(L, t)$, values of their time derivative are estimated from

$$\frac{\partial S(L,t)}{\partial t} = \frac{S(L,t_{i+1}) - S(L,t_i)}{t_{i+1} - t_i}$$

or from the derivative of the regression equation $S(L,t) = a + b\ln t$ for each depth L.

Note that the depths of the tensiometer readings are different from those where the soil water content θ was measured. Those differences allow the total soil water potential head

gradient to be estimated at the same depth where θ was measured. As an example, values of the total soil water potential head at depths of 45 and 75 cm are used to estimate the gradient

Depth L	$\frac{\partial S(L,t)}{\partial t}$ (mm·d^{-1})			
(cm)	t = 0.5 d	t = 2 d	t = 5 d	t = 11 d
30	-10.7	-5.0	-1.4	-0.6
60	-25.0	-9.4	-3.3	-1.8
90	-32.4	-12.6	-4.6	-2.3
120	-40.6	-14.5	-5.6	-2.9

at L = 60 cm. Because the values of water flux density at depths L in the above table are average values between times t_i and t_i+1, it is necessary to calculate the average values of total soil water potential head $\overline{\psi}_T$ from values of ψT given in Table 18 for times t_i and t_i+1.

$$\overline{\psi}_T\left[L,\frac{t_i+t_{i+1}}{2}\right]=\frac{\overline{\psi}_T[L,t_i]+\overline{\psi}_T[L,t_{i+1}]}{2}$$

Depth L	$\overline{\psi}_T$ $[L, (t_i + t_i+1)/2]$ (cm)			
(cm)	t = 0.5 d	t = 2 d	t = 5 d	t = 11 d
15	-28.0	-53.5	-84.5	-117.5
45	-61.5	-90.0	-116.5	-146.5
75	-90.5	-120.0	-149.0	-181.5
105	-124.5	-156.5	-189.0	-217.5
135	-156.0	-186.5	-220.5	-252.5

The hydraulic gradients are calculated using the above values of $\overline{\psi}_T$ according to:

$$\frac{\partial\overline{\psi}_T(L,t)}{\partial z}=\frac{\overline{\psi}_T[L_{j+1},t]-\overline{\psi}_T[L_{j-1},t]}{(L_{j+1}-L_{j-1})}$$

Depth L	$\frac{\partial \overline{\psi}_T(L,t)}{\partial z}$ (cm·cm^{-1})			
(cm)	t = 0.5 d	t = 2 d	t = 5 d	t = 11 d
30	-1.117	-1.217	-1.067	-0.967
60	-0.967	-1.000	-1.083	-1.167
90	-1.133	-1.217	-1.333	-1.200
120	-1.050	-1.000	-1.050	-1.167

We obtain values of the hydraulic conductivity by dividing the soil water flux densities by the respective hydraulic gradients.

Depth L	K (mm·d^{-1})			
(cm)	t = 0.5 d	t = 2 d	t = 5 d	t = 11 d
30	9.58	4.11	1.31	0.62
60	25.85	9.40	3.05	1.54
90	28.60	10.35	3.45	1.92
120	38.67	14.50	5.33	2.48

Values of $\bar{\theta}$ corresponding to the above values of K are calculated from $\theta[L, (t_i + t_{i+1})/2]$ using values of θ given in Table 17.

Depth L	$\bar{\theta}(L, t)$ (cm^3·cm^{-3})			
(cm)	t = 0.5 d	t = 2 d	t = 5 d	t = 11 d
30	0.483	0.449	0.423	0.406
60	0.431	0.390	0.361	0.327
90	0.464	0.445	0.430	0.418
120	0.475	0.458	0.446	0.433

Hence, values of K corresponding to θ for each soil depth L are tabulated together.

$L = 30$		$L = 60$		$L = 90$		$L = 120$	
K	θ	K	θ	K	θ	K	θ
9.58	0.483	25.85	0.431	28.60	0.464	38.67	0.475
4.11	0.449	9.40	0.390	10.35	0.445	14.50	0.458
1.31	0.423	3.05	0.361	3.45	0.430	5.33	0.446
0.62	0.406	1.54	0.327	1.92	0.418	2.48	0.433

For each soil depth L, we perform a regression of $\ln K$ versus θ to ascertain the appropriateness of assuming the functional relation given by equation (68).

Depth L (cm)	Regression equation $\ln K = a + b \cdot \theta$	R^2
30	$\ln K = -14.879 + 35.76\theta$	0.980
60	$\ln K = -8.803 + 28.00\theta$	0.987
90	$\ln K = -24.517 + 60.129\theta$	0.995
120	$\ln K = -27.993 + 66.711\theta$	0.995

Owing to the large values of R^2, we assume that the relation between K and θ is exponential of the form of equation (68) with its parameters K_0, γ and θ_0 determined at depths L.

Depth L (cm)	K_0 (mm·d^{-1})	γ	θ_0 (cm^3·cm^{-3})
30	18.13	35.76	0.501
60	55.65	28.00	0.458
90	57.04	61.13	0.475
120	83.89	66.71	0.486

Owing to the fact that K is exponential function of θ, small errors in the measurement of θ lead to large errors in K.

4.3.2. Libardi et al. (1980) Method

Because this method is based on the assumption that the gradient of the total soil water potential head is unity, the data obtained from tensiometers shown in Table 18 are neglected. Values of K_0 and γ of equation (68) are obtained directly from graphs of $(\theta - \theta_0)$ versus ln$t$ for any given depth L according to the equation:

$$\theta - \theta_0 = \frac{1}{\gamma}\ln t + \frac{1}{\gamma}\ln\left(\frac{\gamma K_0}{L}\right). \qquad (70)$$

Note for depth L that θ_0 is the value of the measured soil water content during steady state infiltration and that K_0 and γ are parameters selected to describe the redistribution process.

Example:

For the measured values of θ_0 at time t = 0 given in Table 17, linear regression equations of graphs of $(\theta - \theta_0)$ versus ln$t$ for each depth L were determined.

Depth L (cm)	Regression equation $(\theta - \theta_0) = a + b \cdot \ln t$	R^2
30	$(\theta - 0.501) = - 0.0376 - 0.0250 \ln t$	0.989
60	$(\theta - 0.458) = - 0.0485 - 0.0354 \ln t$	0.976
90	$(\theta - 0.475) = - 0.0218 - 0.0147 \ln t$	0.996
120	$(\theta - 0.486) = - 0.0207 - 0.0136 \ln t$	0.990

According to equation (70), the slope $b = \gamma^{-1}$ and the intercept $a = \gamma^{-1} \cdot \ln(\gamma . K_0 \cdot L^{-1})$. Hence, we have the parameters K_0, γ and θ_0 determined at depths L.

Depth L (cm)	K_0 (mm·d^{-1})	γ	θ_0 (cm^3·cm^{-3})
30	33.75	40.00	0.501
60	83.59	28.25	0.458
90	58.29	68.03	0.475
120	74.78	73.53	0.486

4.3.3. Sisson et al. (1980) Method

Because this method is also based on the assumption that the gradient of the total soil water potential head is unity, the data obtained from tensiometers shown in Table 18 are again neglected. Values of K_0 and γ of equation (68) are obtained directly from graphs of $\ln(z \cdot t^{-1})$ versus $(\theta - \theta_0)$ for any given depth L according to the equation:

$$\ln(z \cdot t^{-1}) = \ln(\gamma K_0) + \gamma (\theta - \theta_0) \qquad (71)$$

Example:

For the measured values of θ_0 at $t = 0$ given in Table 17, linear regression equations of graphs of $\ln(z \cdot t^{-1})$ versus $(\theta - \theta_0)$ for depths L are required. The data for those regression calculations for $z = L = 30$ are given as

t (d)	$z \cdot t^{-1}$ (cm·d^{-1})	$\ln(z \cdot t^{-1})$	$\theta - \theta_0$ (cm^3·cm^{-3})
1	30	3.4012	-0.035
3	10	2.3026	-0.069
7	4.286	1.4554	-0.087
15	2	0.6931	-0.103

The results of the regressions are

Depth L (cm)	Regression equation $\ln(z \cdot t^{-1}) = a + b \cdot (\theta - \theta_0)$	R^2
30	$\ln(z \cdot t^{-1}) = 4.875 + 39.614(\theta - \theta_0)$	0.989
60	$\ln(z \cdot t^{-1}) = 5.396 + 27.536(\theta - \theta_0)$	0.976
90	$\ln(z \cdot t^{-1}) = 5.971 + 67.650(\theta - \theta_0)$	0.996
120	$\ln(z \cdot t^{-1}) = 6.280 + 72.811(\theta - \theta_0)$	0.990

According to equation (71), the intercept $a = \ln(\gamma K_0)$ and the slope $b = \gamma$. Hence we have the parameters K_0, γ and θ_0 determined at depths L.

Depth L (cm)	K_0 (mm·d^{-1})	γ	θ_0 (cm^3·cm^{-3})
30	33.05	39.61	0.501
60	80.09	27.54	0.458
90	57.91	67.65	0.475
120	73.31	72.81	0.486

In summary, we notice that the results of the latter two methods gave similar values of the soil water parameters for a given soil depth. And, the values from the Richards et al. method differed from those of the latter owing to the inclusion of the measured values of the hydraulic gradient in the calculations.

4.4. Soil Spatial Variability

Neutron probes are ideal for analyzing the distribution and spatial variability of soil water contents within fields and watersheds. By taking a large number of sampling points with a neutron probe and analyzing their spatial and temporal variances with theories of regionalized variables, a better understanding of processes associated with soil water can be achieved. Studies can be performed with a variety of sampling schemes such as sampling locations being equally or randomly spaced in transects or grids.

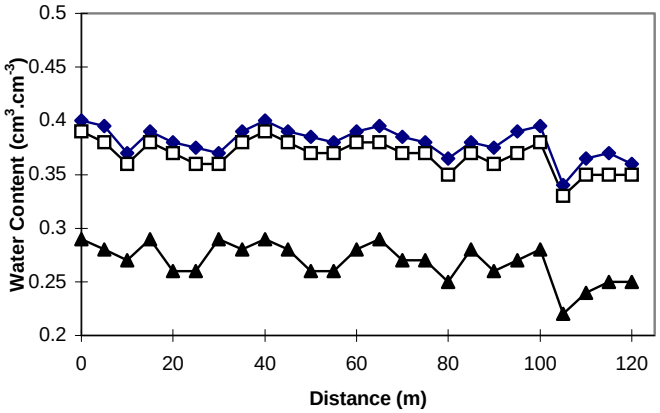

Figure 14 – Soil water content measured on three different dates along a 125-m transect

Figure 14 shows neutron probe measurements of soil water contents taken on three different dates within a transect of 25 access tubes located every 5 m. The nature of the variation of the values along the transect is nearly identical for each of the sampling dates. The coherency of three curves shows that the neutron probe really "samples" the same location at each time (Reichardt et.al., 1993; Reichardt et.al., 1997).

4.5. Water Extraction by Crop Roots

Neutron probes can also be used to examine water extraction patterns of plant roots. Figure 15 shows the spatial distribution of soil water content measured with a neutron probe in a plane beneath two rubber trees (Mendes et al, 1992). Figure 16 shows the spatial distribution of total soil water potential head measured with tensiometers at the same time beneath the same two rubber trees. Although in this case the quantification of soil water flux densities is very difficult, it is possible to draw the directions of water flow which are perpendicular to the isolines of soil water potential head.

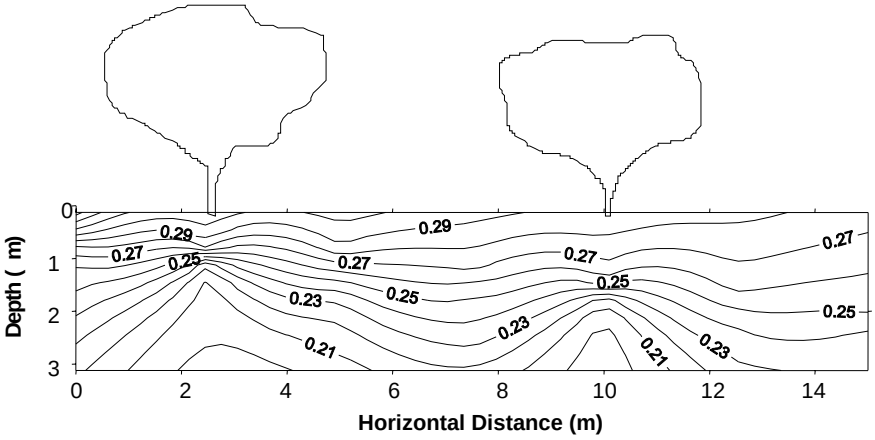

Figure 15 – Isolines of soil water content beneath two rubber trees.

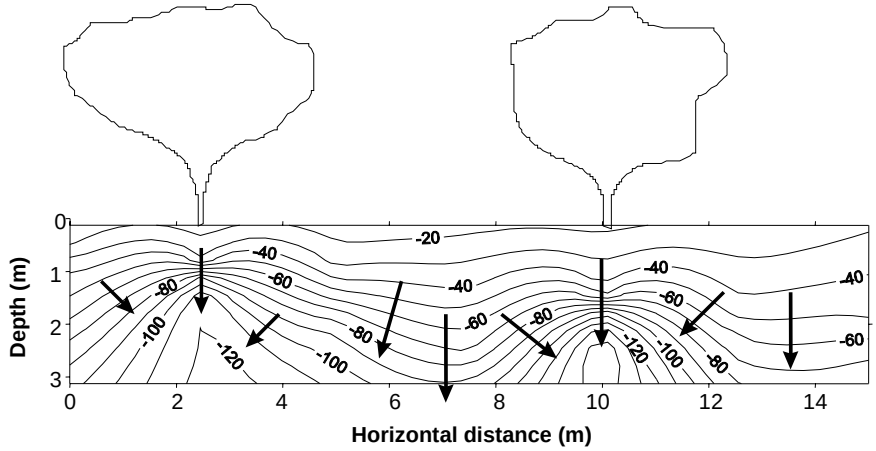

Figure 16 – Isolines of total soil water potential head beneath two rubber trees and water flow directions.

5. References

ARSLAN, A.; RAZZOUK, A.K. and AL-AIN, F. (1997). The performance and radiation exposure of some neutron probes in measuring the water content of the topsoil layer. Aust. J. Soil Res. 35: 1397-1407.

CARNEIRO, C. and DE JONG, E. (1985). In situ determination of the slope of the calibration curve of a neutron probe using a volumetric technique. Soil Sci. 250: 254.

CASSARO, F.A.M., TOMINAGA, T.T., BACCHI, O.O.S., REICHARDT, K., OLIVEIRA,

J.C.M., TIMM, L.C. (2000). Improved calibration of a single-probe surface gamma-neutron gauge. Australian Journal of Soil Research, 38: 937-946.

CASSARO, F.A.M., TOMINAGA, T.T., BACCHI, O.O.S., REICHARDT, K., OLIVEIRA, J.C.M., TIMM, L.C. (2000). The use of a surface gamma-neutron density gauge to explore compacted soil layers. Soil Science, 165: 665-676.

CHASE, G.D. and RABINOWITZ, J.L. (1967). Principles of radioisotope methodology. Third edition. Burgess Publishing Company, Minneapolis, USA.

COUCHAT, P.H.; CARRE, C.; MARCESSE, J. and LEHO, J. (1975). The measurement of thermal neutron constants of the soil: application to the calibration of neutron moisture and the pedological study of the soil. IN: Schrach, R.A., Bowman, C.D. (eds). Nuclear cross sections technology. NBS SP 425: 516.

DOOREMBOS, J. and KASSAM, A.H. (1986). Efectos del agua sobre el rendimiento de los cultivos. IN: FAO. Riego y drenaje. Estudio Nº 33. Rome, Italy.

DOOREMBOS, J. and PRUITT, W.O. (1986). Las necesidades de agua de los cultivos.Roma. IN: FAO. Riego y drenaje. Estudio Nº 24. Rome, Italy.

FALLEIROS, M.C. (1994). Medida da umidade do solo com sonda de nêutrons. Doctor (Thesis) - Instituto de Pesquisas Energéticas e Nucleares, Universidade de São Paulo/CNEN.

GREACEN, E.L. (1981). Soil water assessment by the neutron method. CSIRO, Australia.

GREMINGER, P.J.; SUD, Y.K. and NIELSEN, D.R. (1985). Spatial variability of field measured soil water characteristics. Soil Sci. Soc. Am. J., 49: 1075-82.

GUZMÁN J., M.E. (1989). Nucleonica basica. Segunda edición. Centro de Documentación e Información Nuclear del Instituto de Asuntos Nucleares, Colombia.

HAVERCAMP, R.; VAUCLIN, M. and VACHAUD, G. (1984). Error analysis in estimating soil water content from neutron probe measurement: 1. Local standpoint. Soil Sci., 137: 78-90.

IAEA. (1994). International basic safety standards for protection against ionizing radiation and for the safety of radiation sources. Safety Series Nº 115-I. Vienna, Austria.

IAEA. (1970). Neutron moisture gauges. Technical Report Series Nº 112. Vienna, Austria.

IAEA. (1976). Tracer manual on crops and soils. Technical Report Series Nº 171. Vienna, Austria.

IAEA. (1984). Field soil-water properties measured through radiation techniques. Technical Report Series Nº 312. Vienna, Austria.

IAEA. (1990). Use of nuclear techniques in studies of soil-plant relationships. Training

Course Series Nº 2. Vienna, Austria.

KIRDA, C.; MOUTONNET, P.; HERA, C. and NIELSEN, D.R. (1999). Crop yield response to deficit irrigation. Kluwer Academic Publishers, The Netherlands.

KLUTE, A. (1986). Methods of soil analysis - Part 1- Physical and mineralogical methods. Second edition. SSSA, USA.

KUTÍLEK, M. and NIELSEN, D.R. (1994). Soil hydrology. Catena-Verlag, Germany.

LIBARDI, P.L.; REICHARDT, K.; NIELSEN, D.R. and BIGGAR, J.W. (1980). Simplified field methods for estimating the unsaturated hydraulic conductivity. Soil Sci. Soc. Am. J. 44: 3-6.

MENDES, M.E.G.; VILLAGRA, M.M.; SOUZA, M.D.; BACCHI, O.O.S. and REICHARDT, K. (1992). Relações hídricas em seringal no município de Piracicaba. Sci. Agric. 49(1): 103-109.

NIELSEN, D.R.; DAVIDSON, J.M.; BIGGAR, J.W. and MILLER, R.J. (1964). Water movement through Panoche clay loam soil. Hilgardia 35 (17): 491-506.

OLGAARD, P.L. (1969). Problems connected with the use of subsurface neutron moisture gauges and their solution. Riso-M980 20. Danish Atomic Energy Commission, Denmark.

REICHARDT, K.; BACCHI, O.O.S.; VILLAGRA, M.M.; TURATTI, A.L. and PEDROSA, Z. (1993). Hydraulic variability in space and time in a dark red latosol of the tropics. Geoderma 60: 159-168.

REICHARDT, K.; PORTEZAN, O.; BACCHI, O.O.S.; OLIVEIRA, J.C.M.; DOURADO NETO, D.; PILOTTO, J.E. and CALVACHE, M. (1997). Correção da calibração de sonda de nêutrons por meio de parâmetros de estabilidade temporal da distribuição de probabilidade do conteúdo de água no solo. Sci. Agric. 54 (nº esp.): 17-21.

REICHARDT, K.; ANGELOCCI, L.R.; BACCHI, O.O.S. and PILOTTO, J.E. (1995). Variabilidade diária da chuva em uma escala local (1000ha) em Piracicaba, S.P., e suas implicações na recarga da água do solo. Sci. Agric. 52(1): 43-49.

RICHARDS, L.A.; GARDNER, W.R. and OGATA, G. (1956). Physical processes determining water loss from soil. Soil Sci. Soc. Am. Proc. 20: 310-314.

ROSE, C.W.; STERN, W.R. and DRUMMOND, J.E. (1965). Determination of hydraulic conductivity as a function of depth and water content for soil in situ. Aust. J. Soil Res. 3: 1-9.

SISSON, J.B.; FERGUSON, A.H. and VAN GENUCHTEN, M.Th. (1980). Simple method for predicting drainage from field plots. Soil Sci. Soc. Am. J. 44: 1147-1152.

TIMM, L.C., OLIVEIRA, J.C.M., TOMINAGA, T.T., CASSARO, F.A.M., REICHARDT,

K., BACCHI, O.O.S. (2000). Soil hydraulic conductivity measurement on a sloping field. Brazilian Journal of Agricultural and Environmental Engineering, 4: 480-482.

VAN BAVEL, C.H.M.; STIRK, G.A. and BRUST, K.J. (1968). Hydraulic properties of a clay loam soil and the field measurement of water uptake by roots: 1. Interpretation of water content and pressure profiles. Soil Sci. Soc. Am. Proc. 32: 310-317.

VACHAUD, G.; ROYER, J.M. and COOPER, D. (1977). Comparison of methods of calibration of a neutron probe by gravimetry or neutron capture model. J. Hydrol. 34: 343-356.

VAUCLIN, M.; HAVERCAMP, R. and VACHAUD, G. (1984). Error analysis in estimating soil water content from neutron probe measurements: 2. Spatial standpoint. Soil Sci. 137: 141-148.

VILLAGRA, M.M.; MATSUMOTO, O.M.; BACCHI, O.O.S.; MORAES, S.O.; LIBARDI, P.L. and REICHARDT, K. (1988). Tensiometry and spatial variability in Terra Roxa Estruturada. R. Bras. Ci. Solo, 12: 205-10

VILLAGRA, M.M.; BACCHI, O.O.S.; TUON, R.L. and REICHARDT, K. (1995). Difficulties of estimating evapotranspiration from the water balance equation. Agr. Forest Meteorol. 72: 317-325.

WATSON, K.K. (1966). An instantaneous profile method for determining the hydraulic conductivity of unsaturated porous materials. Water Resour. Res. 2: 709-715.